arXiv:1302.2680v1 [cond-mat.str-el] 12 Feb 2013

Phase diagram of SU(2) composite fermions

Alexander C. Archer and Jainendra K. Jain
Department of Physics, 104 Davey Lab, Pennsylvania State University, University Park PA, 16802, USA

(Dated: February 13, 2013)

We consider the spin physics of fractional quantum Hall effect as a continuous function of the filling factor, and predict a rich phase diagram with magnetic phase transitions whose phase boundaries cut across many fractional plateaus. The calculated phase diagram also applies to fractional quantum Hall effect in systems where valleys may play the role of spin, such as AlAs quantum wells, graphene, and H terminated Si(111) surface.

PACS numbers: 73.43.Cd, 71.10.Pm

The interplay between the Coulomb interaction and the electron spin degree of freedom has led to remarkably rich physics in the fractional quantum Hall effect[1] (FQHE). Phase transitions have been observed as a function of the Zeeman energy, E_Z, in transport,[2–6] optical[7–10] and NMR experiments,[11–15] establishing that, in general, FQHE states with several discrete values of polarization can occur at a given filling factor. The basic physics is understood. The FQHE at filling factor $\nu = n/(2n \pm 1)$ is a manifestation of the integer quantum Hall effect (IQHE) of composite fermions at filling n. For $n > 1$, several states with $n = n_\uparrow + n_\downarrow$ are available, with polarization $P = (n_\uparrow - n_\downarrow)/(n_\uparrow + n_\downarrow)$. Which of these states is favored as a function of E_Z has been determined in detailed microscopic calculations within the composite fermion (CF) theory,[16–18] and can qualitatively be understood in terms of a competition between the Zeeman and the CF cyclotron energies.

The above physics carries over to FQHE in systems with two valleys (with the actual spin frozen due to large Zeeman energy), with the valleys playing the role of spin and the valley splitting of E_Z. Transitions between differently valley polarized CF states have been seen in AlAs quantum wells,[19] where the valley splitting is controlled by application of an in-plane strain. In high quality H-terminated Si(111) surface with two degenerate valleys, the $2 - n/(2n \pm 1)$ states with $n = 2, 4, 6$ have been observed but those with odd n are absent.[20] This behavior is consistent with what is expected in the limit of vanishing valley splitting[16]; if one neglects the residual interaction between composite fermions, a gapped state occurs only for even n. In graphene as well, an effectively two-component CF physics is observed in certain regimes; e.g. the experiments of Refs. 21 and 22 show that in the range $1 < \nu < 2$ FQHE occurs at $2 - n/(2n \pm 1)$ for $n = 2, 4$ but not for odd n (although both even and odd n are observed for $\nu < 1$). Our calculations and results below apply to FQHE in any system where two components are active, but we will use, for simplicity, the convenient language of "spin" and "Zeeman energy."

Theoretically, to date, the SU(2) physics of only the FQHE states at the discrete filling factors $n/(2n \pm 1)$ has been studied.[16–18] In this Letter we obtain the phase diagram as a continuous function of the filling factor. This brings out the fuller richness of the spin physics and reveals additional phase transitions. Further investigation of this phase diagram and the nature of the associated phase transitions should produce deeper insight into the underlying physics of the FQHE.

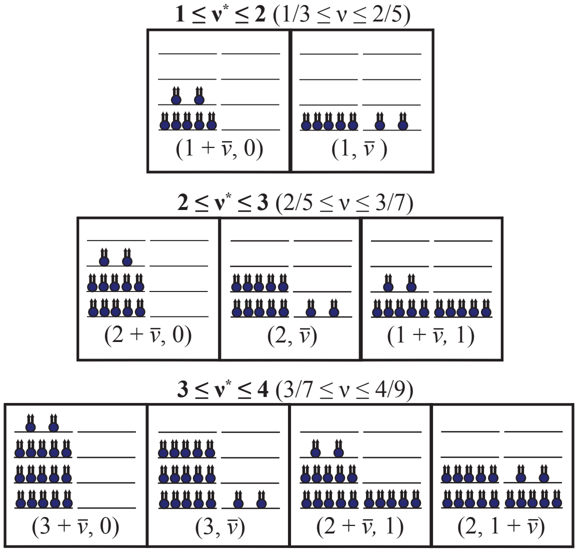

FIG. 1. Schematic description of the states with different polarizations in the filling factor range $1 > \nu^* > 2$ (top), $2 > \nu^* > 3$ (middle) and $3 > \nu^* > 4$ (bottom). Composite fermions are pictured as electrons carrying two arrows (representing bound vortices). The horizontal lines depict the CF ΛLs, with the spin-up ΛLs on the left and spin-down ΛLs on the right. The states are labeled $(\nu^*_\uparrow, \nu^*_\downarrow)$; the filing factor of the partially filled Λ level is $\bar{\nu}$.

At an arbitrary filling in the range $1/3 \le \nu \le 2/3$, electrons capture two vortices to transform into composite fermions,[23,24] which form Landau-like levels called Λ levels (ΛLs), and have a filling factor ν^* given by $\nu = \nu^*/(2\nu^* \pm 1)$. We allow occupation of spin-up and spin-down ΛLs, with $\nu^* = \nu^*_\uparrow + \nu^*_\downarrow$. The corresponding state, labeled $(\nu^*_\uparrow, \nu^*_\downarrow)$, has spin polarization $P = (\nu^*_\uparrow - \nu^*_\downarrow)/\nu^*$. (We take below the convention in which the up spin is favored by the Zeeman energy, i.e., $\nu^*_\uparrow \ge \nu^*_\downarrow$.) We will make the assumption, valid for weakly interacting composite fermions, that only one of the ΛLs is partially occupied, so one of $\nu^*_\uparrow$ and $\nu^*_\downarrow$ is an integer

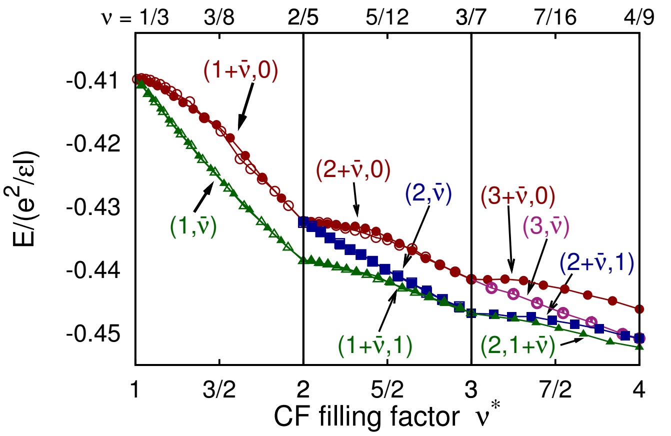

FIG. 2. The total energies of various states $(\nu^*_\uparrow, \nu^*_\downarrow)$ in the filling factor range $1/3 < \nu < 4/9$. The energy E is quoted in units of $e^2/\epsilon\ell$, where $\ell = \sqrt{\hbar c/eB}$ is the magnetic length and ϵ is the dielectric constant of the background material. The dark (open) symbols correspond to states in which the partially filled ΛL contains a crystal of CF particles (holes). In this and subsequent figures, the scale for filling factor is different in the three columnar regions.

and the other will be written as $j + \bar{\nu}$, where $\bar{\nu}$ is the filling factor of the partially filled ΛL. Fig. 1 depicts the possible states between 1/3 and 4/9 studied below.

The wave function of the state $(\nu^*_\uparrow, \nu^*_\downarrow)$ is given by[23]

$$\Psi_\nu = A[\Psi^{\rm CF}_{\nu^*_\uparrow,\nu^*_\downarrow}\{z_1,\cdots z_N\}u_1\cdots u_{N_\uparrow}d_{N_\uparrow+1}\cdots d_N] \quad (1)$$

$$\Psi^{\rm CF}_{\nu^*_\uparrow,\nu^*_\downarrow} = P_{\rm LLL}\prod_{j<k=1}^{N}(z_j - z_k)^2\Phi_{\nu^*_\uparrow,\nu^*_\downarrow} \quad (2)$$

$$\Phi_{\nu^*_\uparrow,\nu^*_\downarrow} = \Phi_{\nu^*_\uparrow}\{z_1,\cdots z_{N_\uparrow}\}\Phi_{\nu^*_\downarrow}\{z_{N_\uparrow+1}\cdots z_N\} \quad (3)$$

Here $z_j = x_j + iy_j$ denotes the position of an electron; $\Phi_{\nu^*_\uparrow}$ and $\Phi_{\nu^*_\downarrow}$ are wave functions of spin up and spin down fermions at $\nu^*_\uparrow$ and $\nu^*_\downarrow$; u and d are the up and down spin spinors; A indicates antisymmetrization; and $P_{\rm LLL}$ denotes lowest Landau level (LLL) projection. For the states relevant to our current study (Fig. 1), all occupied orbitals of spin-down electrons in $\Phi_{\nu^*_\downarrow}$ are definitely occupied for spin-up electrons $\Phi_{\nu^*_\uparrow}$; the product wave function $\Phi_{\nu^*_\uparrow,\nu^*_\downarrow}$ is therefore annihilated by the spin lowering operator (i.e., it satisfies the Fock condition[24]) and is thus an eigenstate of both S_z and $\vec{S}^2$ with $S = S_z$. These properties are preserved[24] under composite fermionization via Eqs. 1 and 2. The LLL projection will be carried out using the method described elsewhere in the literature.[25] The interaction energy

$$E = \frac{\langle\Psi_\nu|V|\Psi_\nu\rangle}{\langle\Psi_\nu|\Psi_\nu\rangle} = \frac{\langle\Psi^{\rm CF}_{\nu^*_\uparrow,\nu^*_\downarrow}|V|\Psi^{\rm CF}_{\nu^*_\uparrow,\nu^*_\downarrow}\rangle}{\langle\Psi^{\rm CF}_{\nu^*_\uparrow,\nu^*_\downarrow}|\Psi^{\rm CF}_{\nu^*_\uparrow,\nu^*_\downarrow}\rangle} \quad (4)$$

where V is the interaction, will be evaluated by the method of Metropolis Monte Carlo.

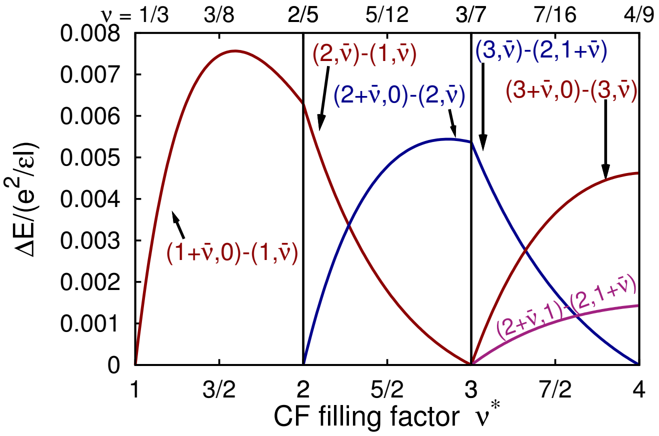

FIG. 3. Difference between the energies of the states with different polarizations, shown near each line, in the filling factor range $1/3 < \nu < 4/9$.

Before proceeding further it is necessary to know the state of composite fermions in the partially filled ΛL (as is the case for one of the two spins), the nature of which is dictated by the weak residual interaction between composite fermions. Close to integer values of ν^*, we expect the formation of a crystal of CF particles or holes. We will assume that the CF crystal is an adequate model for the entire range $0 < \bar{\nu} < 1$, and for completeness, we will consider both the CF particle and CF hole crystals for the entire range. It is possible that some other state of composite fermions (a FQHE liquid, a stripe phase, a paired sate, or a crystal[26]) may have a slightly lower energy than the CF crystal at some intermediate fillings, but we will argue below that the energy differences between such states at a given spin polarization are small compared to the energy differences between differently polarized states, and therefore can be neglected when our primary focus is on the spin polarization of the state.

We will use the spherical geometry[27] for our calculation, in which N electrons are confined to the surface of a sphere with $2Q$ flux quanta passing through it. This geometry is convenient as it has no complications due to edges and enables a simple treatment of the interaction with the background charge (taken as a single positive charge at the center). The crystal of composite fermions is obtained by placing them at the positions that minimize the Coulomb energy of classical charged particles, according to J.J. Thomson's famous plum pudding model of the atom (these positions are tabulated in the literature[28]); as one may expect, this is essentially a triangular crystal with a few defects introduced by the curvature of the spherical surface.

The technical details are as follows. The wave functions for the CF particle or hole crystal at $\nu^* = j + \bar{\nu}$ is constructed from the analogous electron or hole crystal at $\nu = j + \bar{\nu}$. We indicate the electron coordinates variously as $\vec{r} = (\theta, \phi) = (u, v)$, where the spinor variables are defined as $u = \cos(\theta/2)e^{i\phi/2}, v = \sin(\theta/2)e^{-i\phi/2}$. For the electron crystal, we construct the Slater determinant wave function $\Phi_{\nu^*=j+\bar{\nu}}$ with j Landau levels (LLs) completely occupied, and electrons in the partially filled $(j+1)^{\text{th}}$ LL localized at crystal locations. The wave function of an electron wave packet in the $(j+1)^{\text{th}}$ LL (where $j=0$ is the LLL) localized at (U,V) is given by[29]

$$\psi^{2Q}_{(U,V),j} = (S^-)^j \psi^{2(Q+j)}_{(U,V),0} \tag{5}$$

where $\psi^{2Q}_{(U,V),0} = (U^*u + V^*v)^{2Q}$ is the wave function of an electron wave packet localized at (U,V) in the LLL, and $S^- = v^*\partial/\partial u - u^*\partial/\partial v$ is the LL raising operator (which also lowers the monopole strength by a single unit). For the hole crystal, we first construct a Slater determinant wave function $\Phi_{j+1}(\vec{r}_1, \vec{r}_2, \cdots, \vec{r}_{M-1}, \vec{r}_M)$ of $j+1$ filled LLs. Creation of $M-N$ holes localized at $\vec{R}_1, \cdots, \vec{R}_{M-N}$ is accomplished by the action of $\hat{\Psi}(\vec{R}_1)\cdots\hat{\Psi}(\vec{R}_{M-N})$, which produces $\Phi_{j+1}(\vec{r}_1, \vec{r}_2, \cdots, \vec{r}_N, \vec{R}_1, \cdots, \vec{R}_{M-N})$, i.e. $M-N$ electron coordinates are replaced by variables denoting the hole positions. This wave function, however, also produces holes in the lower LLs. That can be taken care of by replacing in the Slater determinant the entries $\chi(\vec{R})$ corresponding to lower LLs by zero, which guarantees that the wave function has holes only in the topmost LL. For example, the wave function Φ_2 with two holes at $\vec{R}_1 = (U_1, V_1)$ and $\vec{R}_2 = (U_2, V_2)$ in the 2nd LL is given by:

$$\Phi_{1+\bar{\nu}} = \begin{vmatrix} v_1^{M/2-2} & \dots & v_N^{M/2-2} & 0 & 0 \\ v_1^{M/2-3}u_1 & \dots & v_N^{M/2-3}u_N & 0 & 0 \\ v_1^{M/2-4}u_1^2 & \dots & v_N^{M/2-4}u_N^2 & 0 & 0 \\ \vdots & & \vdots & \vdots & \vdots \\ u_1^{M/2-2} & \dots & u_N^{M/2-2} & 0 & 0 \\ v_1^{M/2-1}u_1^* & \dots & v_N^{M/2-1}u_N^* & V_1^{M/2-1}U_1^* & V_2^{M/2-1}U_2^* \\ \vdots & & \vdots & \vdots & \vdots \\ u_1^{M/2-1}v_1^* & \dots & u_N^{M/2-1}v_N^* & U_1^{M/2-1}V_1^* & U_2^{M/2-1}V_2^* \end{vmatrix} \tag{6}$$

With these wave functions we construct $\Phi_{\nu^*_\uparrow,\nu^*_\downarrow}$, and substitute in Eq. 2 to get $\Psi^{\text{CF}}_{\nu^*_\uparrow,\nu^*_\downarrow}$. While the full form of the LLL projected Ψ^{CF} is rather complex, it is well defined and produces accurate results.

Fig. 2 shows the Coulomb energies of the various states as a function of the filling factor in the range $1/3 < \nu < 4/9$. The filled (open) symbols represent the energies for states where the partially filled ΛL is modeled as a crystal of CF particles (holes). (In the range $3/7 > \nu > 4/9$ only the CF particle crystal has been evaluated.) The energies are shown for a system with $N = 84$ particles, but we have confirmed, by studying various N values, that the $N = 84$ results are close to the thermodynamic limit. The energies include the interaction with the uniform positive background. The energy difference between the CF particle and hole crystals for a given polarization P is small compared to that between states with different polarizations. Fig. 3 depicts the energy differences between two consecutive states, where we take the lower of the particle or hole crystal energies for a given spin polarization. From the difference, it is straightforward to determine the critical $E_{\text{Z}} \equiv \kappa(e^2/\epsilon\ell)$ for the various transitions, plotted in Fig. 4. (In both Figs. 3 and 4 the curves have been smoothened to eliminate fluctuations due to finite system size. The uncertainty in the curves due to finite size effects is estimated to be $\delta\kappa \approx 0.001$.) The phase diagram in Fig. 4 is the main result of our paper.

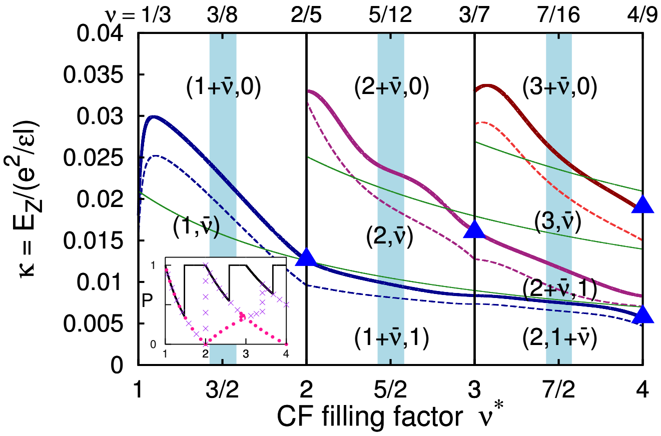

FIG. 4. The calculated polarization phase diagram of various states $(\nu^*_\uparrow, \nu^*_\downarrow)$ in the CF filling factor range $1 < \nu^* < 4$ $(1/3 < \nu < 4/9)$ as a function of $\kappa = E_{\text{Z}}/(e^2/\epsilon\ell)$. The thick solid lines are for a system of zero thickness; the thin dashed lines correspond to a quantum well width of 40 nm for density 10^{11}cm^{-2}; and thin green lines indicate the phase boundaries predicated by a model of noninteracting composite fermions. The shaded regions schematically depict fillings where transitions take place from one plateau to the next. The inset shows the polarization $P = (\nu^*_\uparrow - \nu^*_\downarrow)/\nu^*$ as a function of ν^* for fixed values of $\kappa = 0.0225$ (black solid line), 0.0125 (purple crosses) and 0.005 (red circles), as evaluated for a zero thickness sample without disorder. The blue triangles indicate the spin phase transitions at $\nu^* = n$ identified previously.[17]

The most striking feature of the phase diagram is the presence of lines that cut across many FQHE plateaus. A free-CF model provides useful insight into the structure of the phase diagram. This model considers noninteracting composite fermions, with the CF cyclotron energy taken as[24,30] $\hbar\omega_c^* = \frac{m_e}{m_p^*}\frac{\hbar\omega_c}{2\nu^*\pm1} \equiv \frac{1}{\alpha(2\nu^*\pm1)}\frac{e^2}{\epsilon\ell}$ at $\nu = \frac{\nu^*}{2\nu^*\pm1}$, where $\omega_c = eB/m_ec$ is the cyclotron energy, m_e is the electron mass in vacuum, and m_p^* is the CF "polarization mass."[7,11,17] (For GaAs parameters, we have $m_p^*/m_e = 0.026\alpha\sqrt{B[T]}$.) This model predicts that the phase boundaries between the different polarizations are simply given by $E_{\text{Z}} = \text{integer} \times \hbar\omega_c^*$:

$$\kappa = \frac{\text{integer}}{\alpha(2\nu^*\pm1)} \quad \text{(free CF model)} \tag{7}$$

where the integer goes from 1 to int(ν^*). We show the phase diagram predicted by the free-CF model in Fig. 4 (thin lines), fixing $\alpha = 15.9$ by requiring coincidence at the lower transition at $\nu = 2/5$. (The polarization mass is known to be much larger than the "activation mass" relevant for transport experiments.[7,11,17]) The free CF model reproduces the qualitative features of the phase diagram obtained from the full microscopic theory; the quantitative deviations between the two can be attributed to the residual interaction between composite fermions.

We have also studied the effect of finite thickness assuming a cosine shaped wave function in a square quantum well, which leads to a width dependent effective interaction. As an illustration, the phase diagram is also shown (dashed lines) for a quantum well of width 40 nm at a density of 10^{11} cm^{-2}. Lower densities and shorter widths produce a smaller deviation from the zero width results.

Disorder, not included above, will affect our results in several ways. Most importantly, the first order phase transitions at the phase boundaries will turn into continuous percolation transitions in the presence of disorder, producing extended states that allow identification of the phase transition in transport experiments (below). Disorder will also affect the energies of the various states differently, and thereby modify the phase boundaries. Finally, disorder will create spatial variations in the filling factor, which will provide a correction to the "ideal" polarization. For example, while the ideal 1/3 state is fully spin polarized for all κ, disorder will slightly diminish P for $\kappa < 0.03$. A reliable quantitative estimation of these corrections is not possible at this stage.

For sufficiently large κ, the state is fully polarized at all fillings. Interestingly, for a range of κ values, the state at two consecutive fractions along the sequences $n/(2n+1)$ is fully spin polarized but partially polarized at intermediate fillings. The measurements of Tiemann *et al.* clearly show such behavior where both 1/3 and 2/5 are fully spin polarized but the intermediate state is partially polarized. The inset in Fig. 4 shows the spin polarization $P = (\nu^*_\uparrow - \nu^*_\downarrow)/(\nu^*_\uparrow + \nu^*_\downarrow)$ as a function of ν for several fixed values κ (as would be the case when ν is varied by changing the density at a fixed B), indicating complex κ dependent behavior.

Transport measurements can identify the phase boundary through the appearance of an R_{xx} peak as a function of the E_Z, which appears because of the presence of extended states (due to disorder) at the transition point. These R_{xx} peaks are flanked by two states with the same quantized Hall resistance R_{xy}. (These should be distinguished from the peaks at[31] $\nu^* = n + 1/2$, shown schematically as vertical shaded regions in Fig. 4, which indicate transition between states with different values of the Hall resistance.) Such peaks have been seen in a number of experiments, both at the special fractions $\nu = n/(2n \pm 1)$ and slightly away from it.[2,3,5,13] Krauss *et al.*[13] have detected a sharp R_{xx} peak inside the resistance minima near 2/3 and 3/5, and determined a phase boundary of the type calculated here, clearly delineating states with various spin polarizations as a function of the filling factor. Unfortunately, a technical difficulty in dealing with reverse flux attachment makes the calculation of the phase diagram along the sequence $n/(2n-1)$ much more challenging,[16,18] and outside the scope of the present work. However, the phase transition at 2/3 is found to occur in Ref. 13 at $\sim 10T$, which, according to the free CF model, corresponds to $\alpha \sim 19$, which is in the same ball park as the value obtained above (and, in fact, somewhat higher, as expected from finite width corrections). Resistance spikes have also been observed at magnetic phase transitions in the integer quantum Hall regime.[32] We also note that because the phase boundary involves a change of magnetization, it should exhibit hysteretic behavior, as observed previously.[3,5,12,32]

Before ending, we note that we have focused here on magnetic transitions, and not attempted to discriminate between various possible states of composite fermions with the same spin polarization, such as their FQHE, paired state, stripes or crystals.[26] The difference between the energies of such states for a given spin polarization is likely to be much less than that between the states of different spin polarizations, as evidenced by the relatively small difference between the energies of the CF particle and hole crystals. A more detailed phase diagram will contain additional phase boundaries separating different states with the same spin polarization. Further, for graphene and other multi-valley systems, it will be important to consider both the spin and valley indices to bring out the full physics.[21,33]

We thank the National Science Foundation for support under grant no. DMR-1005536, and the Research Computing and Cyberinfrastructure, a unit of Information Technology Services at Pennsylvania State University, for providing high-performance computing resources.

---

[1] D.C. Tsui, H.L. Stormer, and A.C. Gossard, Phys. Rev. Lett. **48**, 1559 (1982).

[2] R. R. Du *et al.*, Phys. Rev. Lett. **75**, 3926 (1995).

[3] H. Cho *et al.*, Phys. Rev. Lett. **81**, 2522 (1998).

[4] A. S. Yeh *et al.*, Phys. Rev. Lett. **82**, 592 (1999)

[5] J. Eom *et al.*, Science **289**, 2320 (2000).

[6] B. A. Piot *et al.*, Phys. Rev. B **82**, 081307 (2010); C. Betthausen *et al.*, preprint.

[7] I. V. Kukushkin, K. v. Klitzing and K. Eberl, Phys. Rev. Lett. **82**, 3665 (1999); I. V. Kukushkin, J. H. Smet, K. von Klitzing, and K. Eberl, *ibid.* **85**, 3688 (2000).

[8] G. Yusa, H. Shtrikman, and I. Bar-Joseph, Phys. Rev. Lett. **87**, 216402 (2001).

[9] G. Groshaus, P. Plochocka-Polack, M. Rappaport, V. Umansky, I. Bar-Joseph, B. S. Dennis, L. N. Pfeiffer, K. W. West, Y Gallais, and A. Pinczuk, Phys. Rev. Lett. **98**, 156803 (2007).

[10] J. Hayakawa, K. Muraki and G. Yusa, Nat. Nano. **8**, 31

(2013).

[11] S. Melinte *et al.*, Phys. Rev. Lett. **84**, 354 (2000); N. Freytag *et al.*, *ibid.* **89**, 246804 (2002).

[12] J. H. Smet *et al.*, Phys. Rev. Lett. **86**, 2412 (2001).

[13] S. Kraus *et al.*, Phys. Rev. Lett. **89**, 266801 (2002).

[14] J. H. Smet *et al.*, Phys. Rev. Lett. **92**, 086802 (2004).

[15] L. Tiemann, G. Gamez, N. Kumuda and K. Muraki, Science **335**, 828 (2012).

[16] X.G. Wu, G. Dev, and J.K. Jain, Phys. Rev. Lett. **71**, 153 (1993).

[17] K. Park and J. K. Jain, Phys. Rev. Lett. **80**, 4237 (1998); *ibid.* **83**, 5543 (1999).

[18] S.C. Davenport and S.H. Simon, Phys. Rev. B **85**, 245303 (2012).

[19] N. C. Bishop, M. Padmanabhan, K. Vakili, Y.P. Snokolnikov, E. P. De Poortere, and M. Shayegan, Phyr. Rev. Lett. **98**, 266404 (2007); M. Padmanabhan, T. Gokmen, M. Shayegan, Phys. Rev. B **80**, 035423 (2009); Phys. Rev. B **81**, 113301 (2010); T. Gokmen, M. Padmanabhan, and M. Shayegan, Nature Physics **6**, 621 (2010).

[20] T.M. Kott, B. Hu, S. H. Brown, and B. E. Kane, arXiv:1210.2386 (2012).

[21] C. R. Dean *et al.*, Nat. Phys. **7**, 693 (2011).

[22] B. E. Feldman, B. Krauss, J. H. Smet and A. Yacoby, Science **337**, 1196 (2012).

[23] J.K. Jain, Phys. Rev. Lett. **63**, 199 (1989); Phys. Rev. B **41**, 7653 (1990).

[24] Jainendra K. Jain, *Composite Fermions* (Cambridge University Press, Cambridge, UK, 2007).

[25] J.K. Jain and R.K. Kamilla, Phys. Rev. B **55**, R4895 (1996); Int. J. Mod. Phys. B **11**, 2621 (1997).

[26] S. Y. Lee,V. W. Scarola, and J. K. Jain, Phys. Rev. Lett. **87**, 256803 (2001); Phys. Rev. B **66**, 085336 (2002); V. W. Scarola, J. K. Jain, E. H. Rezayi, Phys. Rev. Lett. **88**, 216804 (2002); C.-C. Chang, S. S. Mandal and J. K. Jain, Phys. Rev. B **67**, 121305(R) (2003); M. O. Goerbig, P.Lederer, and C.M. Smith, Phys. Rev. B **69**, 155324 (2004); A. Wójs, K.-S. Yi, and J. J. Quinn, Phys. Rev. B **69**, 205322 (2004); A. Wójs, G. Simion, and J. J. Quinn, Phys. Rev. B **75**, 155318 (2007); S. Mukherjee *et al.*, Phys. Rev. Lett. **109**, 256801 (2012).

[27] F.D.M. Haldane, Phys. Rev. Lett. **51**, 605 (1983).

[28] David J. Wales, Hayley McKay, and Eric L. Altschuler, Phys. Rev. B **79**, 224115 (2009); David J. Wales and Sidika Ulker, Phys. Rev. B **74**, 212101 (2006); M. J. Bowick, C. Cecka, L. Giomi, A. Middleton and K. Zielnicki, http://thomson.phy.syr.edu/thomsonapplet.php.

[29] Martin Greiter, Phys. Rev. B **83**, 115129 (2011).

[30] B. I. Halperin, P. A. Lee, N. Read, Phys. Rev. B **47** 7312 (1993).

[31] V. J. Goldman, J. K. Jain and M. Shayegan, Phys. Rev. Lett. **65**, 907 (1990).

[32] E. P. De Poortere, E. Tutuc, S. J. Papadakis, and M. Shayegan, Science **290**, 1546 (2000).

[33] C. Töke and J. K. Jain, Phys. Rev. B **75**, 245440 (2007); M. O. Goerbig and N. Regnault, Phys. Rev. B **75**, 241405 (2007); N. Shibata and K. Nomura, J. Phys. Soc. Japan **78**, 104708 (2009).